



Contents lists available at ScienceDirect

Journal of King Saud University – Science

journal homepage: www.sciencedirect.com

Original article

Exact solitary wave and numerical solutions for geophysical KdV equation

Abdulghani R. Alharbi, M.B. Almatrafi

Department of Mathematics, College of Science, Taibah University, Al-Madinah Al-Munawarah, Saudi Arabia



ARTICLE INFO

Article history:

Received 26 November 2021

Revised 6 May 2022

Accepted 10 May 2022

Available online 23 May 2022

AMS Subject Classification:

35B07

35B10

35B40

65N06

65E99

65G99

65L07

65L12

65N12

Keywords:

Geophysical Korteweg-de Vries equation

The improved $\exp(-F(\eta))$ -expansion

approach

Stability

Error

Accuracy

Scheme

ABSTRACT

Tsunamis are strong waves, arisen from volcanic eruptions, landslides, or earthquakes sweeping across oceans. The geophysical Korteweg-de Vries (gKdV) equation which governs the tsunami wave propagation in oceans is investigated in this work using an improved $\exp(-F(\eta))$ -expansion method. Shooting and adaptive moving approaches are taken into account. We retrieve several new solitary solutions for the gKdV equation. The obtained solution from implementing shooting method is successfully used as an initial value for the adaptive approach which is utilized to construct the numerical solution of the proposed problem. The constructed exact solutions coincide with the obtained numerical solutions. The accuracy of the presented numerical approximations is discussed. We apply Fourier concept to explore the accuracy and stability of the numerical schemes which is unconditionally stable. A clear comparison between the analytic and numerical outcomes is presented via some 2D and 3D sketches which are depicted under special selections of some parameters. Moreover, we illustrate the relative error and CPU time for the numerical technique. The proposed approaches can be easily utilized to deal with other partial differential equations.

© 2022 The Author(s). Published by Elsevier B.V. on behalf of King Saud University. This is an open access article under the CC BY license (<http://creativecommons.org/licenses/by/4.0/>).

1. Introduction

Research on partial differential equations (PDEs) and relevant topics have been widely increased recently. It has become an active topic in several spheres of engineering, physical and mathematical sciences, particularly, in mechanical engineering, fluid mechanics, traveling waves, plasma physics, fibers, nonlinear optics, signal

processing, control theory, and others. Exact and numerical solutions play an essential role in investigating these phenomena. Over the previous decades, several powerful approaches have been successfully invoked to extract the analytic solutions of nonlinear equations (NLEEs) for instance the homogeneous balance technique (Wang et al., 1996), the improved $\exp(-F(x))$ -expansion method (Chen et al., 2019), the improved Kudryashov approach (Kumar et al., 2018), the first integral technique (Bekir and Unsal, 2012), the Adomian decomposition strategy (Adomian, 1994; Wazwaz, 2002), etc. Soliton solutions may form different types of shapes e.g. S-shaped soliton, kink wave, bell shape, lump wave, M-shaped soliton, peakons, cuspons and some others (Rao et al., 2019; Abdullah and Wang, 2019; Liu and Zhang, 2018; Alharbi and Almatrafi, 2020; Alam and Tunç, 2020; Alharbi and Almatrafi, 2020; Alharbi and Almatrafi, 2020; Özkan et al., 2020; El-Shiekh and Gaballah, 2020; Khater et al., 2020; Almatrafi et al., 2020; Alharbi et al., 2020; Alharbi et al., 2020; Akbar et al.,

E-mail addresses: arharbi@taibahu.edu.sa (A.R. Alharbi), mmutrafi@taibahu.edu.sa (M.B. Almatrafi).

Peer review under responsibility of King Saud University.



Production and hosting by Elsevier

<https://doi.org/10.1016/j.jksus.2022.102087>

1018-3647/© 2022 The Author(s). Published by Elsevier B.V. on behalf of King Saud University. This is an open access article under the CC BY license (<http://creativecommons.org/licenses/by/4.0/>).

2021; Akinyemi et al., 2021; Zafar et al., 2022; Nisar et al., 2021; Houwe et al., 2022; Martínez et al., 2021).

Korteweg-de Vries (KdV) like equations are widely used to describe a massive number of applications in several branches of nonlinear science and engineering. Historically, KdV problem was found by Korteweg and De Vries in 1895 (Korteweg et al., 1895). Then, researchers have introduced many modifications for this equation. For example, Johnson (2002) described a specific approach to find the Camassa-Holm problem in the context of water waves and presented the connection with the KdV equation. In Wazzan (2009), Wazzan successfully applied a modified tanh-coth approach to extract new solutions for the KdV and Korteweg-de Vries-Burgers' problems. Moreover, Kudryashov (2009) analyzed some exact solutions of KdV and KdV-Burgers problems. The Hirota's bilinear technique was used in Wazwaz (2010) to investigate the solutions of the perturbed KdV equation. Triki et al. (2017) applied auxiliary equation approach to extract some soliton-like solutions for a second order wave equation of KdV. The derivation of the gKdV equation was achieved in Geyer and Quirchmayr (2017) using techniques from asymptotic analysis. Some explicit traveling wave solutions for the gKdV equation were presented in Geyer and Quirchmayr (2017) using Jacobi elliptic functions. In Ak et al. (2020), the Coriolis effect on oceanic flows was deeply investigated via the gKdV equation. The propagation of some solitary solutions was produced in Ak et al. (2020). Moreover, the authors implemented the finite element approach to construct numerical simulations for the gKdV equation. The homotopy perturbation technique was used in Karunakar and Chakraverty (2019) to deal with the gKdV equation and develop some analytic solutions. Furthermore, Rizvi et al. (2020) used the Hirota bilinear method to show some lump soliton solutions for gKdV equation.

In this work, we discuss a novel and reputed PDE known as geophysical Korteweg-de Vries equation (Geyer and Quirchmayr, 2017) which is given by

$$\psi_t - \mu\psi_x + \frac{3}{2}\psi\psi_x + \frac{1}{6}\psi_{xxx} = 0, \tag{1}$$

where $\psi = \psi(x, t)$ denotes the free surface advancement and μ represents Coriolis effect parameter which depends on the water depth. Eq. (1) is used as a model for shallow water waves and tsunami wave propagation (Geyer and Quirchmayr, 2017). According to Karunakar and Chakraverty (2019), μ is proportional to the height of the wave and inversely proportional to wavelength. This implies that the existence of Coriolis constant has a significant impact on the shape of the solutions. The essential aims of this paper are to extract novel exact solutions and acceptable numerical approximations for the considered problem by employing the improved $\exp(-F(\eta))$ -expansion method and the adaptive technique, respectively. The shooting method is successfully applied for the proposed equation and its solution is utilized to generate the initial condition of the adaptive moving mesh method. Then, we compare the constructed results with each other to show the validity of the used methods. Moreover, we develop the stability and accuracy of the numerical scheme. Several 3D and 2D sketches are illustrated to exhibit the behavior of the solutions. We also present the error which is resulted from the used numerical method.

The outline of this work is explained in this paragraph. Section 2 presents a summary for the improved $\exp(-F(\eta))$ -expansion technique. In Section 3, we analyze some new solutions for the gKdV problem. In Section 4, we discuss the numerical solution of the relevant equation while Section 5 presents the finite difference, the stability and the accuracy of the numerical approximation. Moreover, Section 6 is added to highlight the outcomes accomplished in this study. Ultimately, Section 7 concludes this article.

2. Methodology

This part is devoted to introduce the improved $\exp(-F(\eta))$ -expansion approach, as given in Chen et al. (2019). Assume that

$$Q(\theta, \theta_x, \theta_t, \theta_{xx}, \theta_{xxx}, \dots) = 0, \tag{2}$$

is a given PDE in the unknown functions $\theta = \theta(x, t)$, $\theta_x, \theta_t, \dots$. Then, insert the transformations

$$\theta(x, t) = V(\xi), \quad \xi = x - h_t, \tag{3}$$

into Eq. (2) to reduce Eq. (2) into an ordinary differential equation (ODE) expressed as

$$\Theta(V, V', V'', V''', \dots) = 0, \tag{4}$$

where $\iota = \frac{d}{d\xi}$. Next, Eq. (4) is integrated term by term and we take the integral constants by zero. According to this technique, the solutions of Eq. (4) are expressed as

$$V(\xi) = \sum_{i=1}^{N+1} a_{i-1} \exp(-(i-1)F(\xi)), \tag{5}$$

where,

$$F_\xi^2 = \beta^2 (r_0 \exp(-2F(\xi)) + r_1 + r_2 \exp(2F(\xi))). \tag{6}$$

The constants β, r_0, r_1, r_2 and a_i ($i = 1, 2, \dots, N + 1$) are obtained later. In order to calculate the value of N , we apply the homogeneous balance. we use some Jacobi elliptic function solutions presented in Chen et al. (2019) for Eq. (5). Next, we plug Eqs. (5) and (6) into Eq. (4) and equate the coefficients of $\exp(-F(\xi))$ to zero to end up with an algebraic system solved by using Mathematica or Maple. The values of the above-mentioned constants are contained in the solutions of this system. Substituting the values of these constants into Eq. (5) yields the exact solutions.

3. Exact solutions

This section explores the solitary wave solutions of the considered problem. Using Eq. (3), we can express Eq. (1) by

$$2V'' + 9V^2 - 12(\delta + \mu)V = 0. \tag{7}$$

We now balance terms to have $N = 2$. Hence, from Eq. (5), we have

$$V(\xi) = a_0 + a_1 \exp(-F(\xi)) + a_2 \exp(-2F(\xi)). \tag{8}$$

Next, we substitute Eq. (8) into Eq. (7) to end up with algebraic equations whose solutions are given by

$$\begin{aligned} a_0 &= \frac{4}{9}\beta^2 \left(-r_1 \pm \sqrt{r_1^2 - 3r_0r_2} \right), \\ a_1 &= 0, \\ a_2 &= -\frac{4\beta^2r_0}{3}, \\ \delta &= \frac{1}{3} \left(-3\mu \pm 2\beta^2 \sqrt{r_1^2 - 3r_0r_2} \right). \end{aligned}$$

Now, when $m \rightarrow 1$, we can obviously develop several exact solutions given as follows. If $r_0 = 1, r_1 = -1 - m^2$ and $r_2 = m^2$. Then, the exact traveling wave solution is given by

$$\begin{aligned} \psi_1 &= \frac{4}{9}\beta^2 \left(-r_1 \pm \sqrt{r_1^2 - 3r_0r_2} \right) \\ &\quad - \frac{4\beta^2r_0}{3} \coth^2 \left(\beta \left(x - \frac{1}{3} \left(-3\mu \pm 2\beta^2 \sqrt{r_1^2 - 3r_0r_2} \right) t \right) \right). \end{aligned}$$

If $r_0 = 1 - m^2, r_1 = -1 + 2m^2$ and $r_2 = -m^2$. Then, the exact traveling wave solutions are given by

$$\psi_2 = \frac{4}{9}\beta^2 \left(-r_1 \pm \sqrt{r_1^2 - 3r_0r_2} \right) - \frac{4\beta^2 r_0}{3} \operatorname{sech}^2 \left(\beta \left(x - \frac{1}{3} \left(-3\mu \pm 2\beta^2 \sqrt{r_1^2 - 3r_0r_2} \right) t \right) \right).$$

If $r_0 = m^2$, $r_1 = -1 - m^2$ and $r_2 = 1$. Then, the exact traveling wave solutions are given by

$$\psi_3 = \frac{4}{9}\beta^2 \left(-r_1 \pm \sqrt{r_1^2 - 3r_0r_2} \right) - \frac{4\beta^2 r_0}{3} \tanh^2 \left(\beta \left(x - \frac{1}{3} \left(-3\mu \pm 2\beta^2 \sqrt{r_1^2 - 3r_0r_2} \right) t \right) \right).$$

If $r_0 = -m^2$, $r_1 = 2m^2 - 1$ and $r_2 = -1 - m^2$. Then, the exact traveling wave solutions are given by

$$\psi_4 = \frac{4}{9}\beta^2 \left(-r_1 \pm \sqrt{r_1^2 - 3r_0r_2} \right) - \frac{4\beta^2 r_0}{3} \cosh^2 \left(\beta \left(x - \frac{1}{3} \left(-3\mu \pm 2\beta^2 \sqrt{r_1^2 - 3r_0r_2} \right) t \right) \right).$$

If $r_0 = 1$, $r_1 = 2 - m^2$ and $r_2 = -1 - m^2$. Then, the exact traveling wave solutions are given by

$$\psi_5 = \frac{4}{9}\beta^2 \left(-r_1 \pm \sqrt{r_1^2 - 3r_0r_2} \right) - \frac{4\beta^2 r_0}{3} \sinh^2 \left(\beta \left(x - \frac{1}{3} \left(-3\mu \pm 2\beta^2 \sqrt{r_1^2 - 3r_0r_2} \right) t \right) \right).$$

If $r_0 = 1 - m^2$, $r_1 = 2 - m^2$ and $r_2 = 1$. Then, the exact traveling wave solutions are given by

$$\psi_6 = \frac{4}{9}\beta^2 \left(-r_1 \pm \sqrt{r_1^2 - 3r_0r_2} \right) - \frac{4\beta^2 r_0}{3} \operatorname{csch}^2 \left(\beta \left(x - \frac{1}{3} \left(-3\mu \pm 2\beta^2 \sqrt{r_1^2 - 3r_0r_2} \right) t \right) \right).$$

Now, when $m \rightarrow 0$, we can clearly obtain several exact solutions given as follows. If $r_0 = 1$, $r_1 = -1 - m^2$ and $r_2 = m^2$. Then, the exact traveling wave solution is given by

$$\psi_1 = \frac{4}{9}\beta^2 \left(-r_1 \pm \sqrt{r_1^2 - 3r_0r_2} \right) - \frac{4\beta^2 r_0}{3} \operatorname{csc}^2 \left(\beta \left(x - \frac{1}{3} \left(-3\mu \pm 2\beta^2 \sqrt{r_1^2 - 3r_0r_2} \right) t \right) \right).$$

If $r_0 = 1 - m^2$, $r_1 = -1 + 2m^2$ and $r_2 = -m^2$. Then, the exact traveling wave solutions are given by

$$\psi_2 = \frac{4}{9}\beta^2 \left(-r_1 \pm \sqrt{r_1^2 - 3r_0r_2} \right) - \frac{4\beta^2 r_0}{3} \times \cos^2 \left(\beta \left(x - \frac{1}{3} \left(-3\mu \pm 2\beta^2 \sqrt{r_1^2 - 3r_0r_2} \right) t \right) \right).$$

If $r_0 = m^2$, $r_1 = -1 - m^2$ and $r_2 = 1$. Then, the exact traveling wave solutions are given by

$$\psi_3 = \frac{4}{9}\beta^2 \left(-r_1 \pm \sqrt{r_1^2 - 3r_0r_2} \right) - \frac{4\beta^2 r_0}{3} \times \sin^2 \left(\beta \left(x - \frac{1}{3} \left(-3\mu \pm 2\beta^2 \sqrt{r_1^2 - 3r_0r_2} \right) t \right) \right).$$

If $r_0 = -m^2$, $r_1 = 2m^2 - 1$ and $r_2 = -1 - m^2$. Then, the exact traveling wave solutions are given by

$$\psi_4 = \frac{4}{9}\beta^2 \left(-r_1 \pm \sqrt{r_1^2 - 3r_0r_2} \right) - \frac{4\beta^2 r_0}{3} \times \sec^2 \left(\beta \left(x - \frac{1}{3} \left(-3\mu \pm 2\beta^2 \sqrt{r_1^2 - 3r_0r_2} \right) t \right) \right).$$

If $r_0 = 1$, $r_1 = 2 - m^2$ and $r_2 = -1 - m^2$. Then, the exact traveling wave solutions are given by

$$\psi_5 = \frac{4}{9}\beta^2 \left(-r_1 \pm \sqrt{r_1^2 - 3r_0r_2} \right) - \frac{4\beta^2 r_0}{3} \times \tan^2 \left(\beta \left(x - \frac{1}{3} \left(-3\mu \pm 2\beta^2 \sqrt{r_1^2 - 3r_0r_2} \right) t \right) \right).$$

If $r_0 = 1 - m^2$, $r_1 = 2 - m^2$ and $r_2 = 1$. Then, the exact traveling wave solutions are given by

$$\psi_6 = \frac{4}{9}\beta^2 \left(-r_1 \pm \sqrt{r_1^2 - 3r_0r_2} \right) - \frac{4\beta^2 r_0}{3} \cot^2 \left(\beta \left(x - \frac{1}{3} \left(-3\mu \pm 2\beta^2 \sqrt{r_1^2 - 3r_0r_2} \right) t \right) \right).$$

4. Numerical solution

We now investigate the numerical solution of Eq. (7) by implementing the nonlinear shooting method. We only take an initial value at x_0 and then we choose an initial guess for the first derivative at x_0 . It is worth known that we use MATLAB sub-routine ODE15s (Shampine and Reichelt, 1994) and modify the parameter until the second boundary condition is satisfied. Moreover, we use the solution obtained by shooting method as an initial condition for the adaptive moving mesh approach which is straightforwardly employed to obtain the numerical solution of the proposed problem. Eq. (7) can be written as

$$f(V) = 0, \quad f(V) = 2V'' + 9V^2 - 12(\delta + \mu)V. \tag{9}$$

It is notable that Eq. (9) is discretized by utilizing the finite difference notations on a fixed mesh resulting in a nonlinear equations system. We solve the resulting system using MATLAB sub-routine FSOLVE (Shampine and Reichelt, 1994) which applies the Quasi-Newton method.

5. Finite difference semi-discretization scheme

In this section, we construct a semi-discretization scheme by executing the adaptive moving mesh process with a finite difference for the numerical solutions of the gKdV equation. This method applies a transformation coordinate from a computational domain $[0, 1]$, to a physical one $[a, b]$. That is

$$x = x(\eta, t) : [0, 1] \rightarrow [a, b], \quad t \in [0, T_e],$$

where $\eta \in [0, 1]$ is a computational coordinate and T_e is a fixed time. Thus, the solution ψ is now dependent on a moving mesh coordinate $x(\eta, t)$. The moving mesh coordinate associated with ψ is given by

$$\begin{cases} x_i(\eta) = x_i(\eta_i, t), & i = 0, 1, 2, \dots, N_x, \\ x_0 = a, & x_{N_x} = b, \\ x_i(\eta_i, 0) = i \frac{b-a}{N_x}, \end{cases}$$

where a and b represent the boundaries of the domain. A computational coordinate is represented as

$$\begin{cases} \eta_i = i \frac{1}{N_x}, & i = 0, 1, 2, \dots, N_x, \\ \eta_0 = 0, & \eta_{N_x} = 1. \end{cases}$$

By applying the chain rule, Eq. (1) is given by

$$\begin{cases} \dot{\psi} = \frac{G_\eta}{x_\eta} + \frac{\psi_\eta}{x_\eta} \dot{x}, \\ G = \mu \frac{\psi_\eta}{x_\eta} - \frac{3}{4} \frac{(\psi^2)_\eta}{x_\eta} - \frac{1}{6x_\eta} \left(\frac{\psi_\eta}{x_\eta} \right)_\eta. \end{cases} \tag{10}$$

In order to establish a new equidistributing mesh, we require to solve the most common moving mesh partial differential equation (MMPDE) given by

$$\tau x_t = (\rho x_\eta)_\eta, \tag{11}$$

where $\tau \in (0, 1)$ indicates a relaxation parameter, and ρ is a mesh density function. This moving mesh equation was originally presented in [Adjerid \(1986\)](#). Eq. (11) is known as MMPDE6 ([Huang et al., 1994](#)). Suppose that a solution $\psi^n = \psi(x^n, t^n)$, and a mesh $x^n = x(t^n)$ are identified at time $t = t^n$. Then, the basic procedure of the considered method to develop the numerical solution of Eq. (10) is implemented in several steps.

1. We compute the mesh density function ρ^n at $t = t^n$ using x^n and ψ^n .
2. We discretize the moving mesh PDE (MMPDE) in a computational coordinate using the central finite differences. Then, we integrate the resulting system over $[t^n, t^{n+1}]$ to obtain a new equidistributing mesh coordinate x^{n+1} . The computation is done by using the function ρ^n . Observe that the solution ψ^n is not developed during this computation.
3. Linear interpolation is used to match the new mesh x^{n+1} with the previous solution ψ^n .
4. The physical PDE (Eq. (10)) is discretized in the new mesh. Then, we integrate the resulting system using an ODE MATLAB solver to obtain the solution ψ^{n+1} . Here, we use ODE15i. ODE15i solver is a MATLAB solver based on the backward-differentiation formulas (BDFs) of the highest order up to 5. This solver is intended to be utilized with fully implicit differential equations (DEs) and differential-algebraic equations (DAEs). In this estimate, we use

$$\dot{x}_i = \frac{x_i^{n+1} - x_i^n}{h_t}.$$

5. Repeat these steps starting from the first step.

In this study, the central finite differences method is invoked to fully discretize the derivatives of the MMPDE6.

$$\tau(x_i^{n+1} - x_i^n) = \alpha \left(\frac{\rho_{i+1}^{n+1} + \rho_i^n}{2} (x_{i+1}^{n+1} - x_i^{n+1}) - \frac{\rho_i^n + \rho_{i-1}^n}{2} (x_i^{n+1} - x_{i-1}^{n+1}) \right), \tag{12}$$

subject to

$$x_0 = a, \quad x_{N_x} = b,$$

with the initial condition

$$x_i(\eta_i, 0) = i \frac{b - a}{N_x},$$

where $\alpha = \frac{h_t}{\tau \rho^n \Delta \eta}$. The resulting system, given in Eq. (12), is integrated to obtain the new equidistributing coordinate transformation $x(\eta, t)$. Furthermore, Eq. (10) is transformed into a semi-discretization for the spatial derivative which can be expressed in the computational coordinate as follows:

$$\begin{cases} \frac{\psi_i^{n+1} - \psi_i^n}{h_t} = \frac{G_i^{n+1} - G_i^{n+1}}{x_{i+1}^{n+1} - x_{i-1}^{n+1}} + \frac{G_i^n - G_i^n}{x_{i+1}^n - x_{i-1}^n} + 0.5 \left(\frac{\psi_{i+1}^{n+1} - \psi_{i-1}^{n+1}}{x_{i+1}^{n+1} - x_{i-1}^{n+1}} + \frac{\psi_{i+1}^n - \psi_{i-1}^n}{x_{i+1}^n - x_{i-1}^n} \right) \dot{x}_i, \\ G_i^n = \mu \psi_i^n - 0.75 \psi_{|i}^2 |i^n - \frac{1}{3(x_{i+1}^n - x_{i-1}^n)} \left(\frac{\psi_{i+1}^n - \psi_i^n}{x_{i+1}^n - x_i^n} - \frac{\psi_i^n - \psi_{i-1}^n}{x_i^n - x_{i-1}^n} \right). \end{cases} \tag{13}$$

Systems (12) and (13) lead to a tridiagonal coefficient matrices which consist of three diagonals and the remaining entries are zeros. Therefore, we use the Crout factorization method to reduce the number of operations and obtain the results at a higher speed.

The advantage of this method is to avoid finding the inverse of the coefficient matrices and only uses the backward substitution. Here, we use MATLAB to obtain the numerical results.

5.1. Accuracy

This part discusses the accuracy of the numerical schemes (12) and (13). The approximation solution ψ_i^n is replaced by $\psi(x_i, t_n)$ at the point (x_i, t_n) . The mesh density function is assumed to be $\rho_i = 1, \forall i = 1, \dots, N_x$. Now, we use Taylor series expansion to expand x_{i+1}^{n+1} and x_{i-1}^{n+1} as follows:

$$\begin{aligned} x_{i+1}^{n+1} &= x_i^{n+1} + \Delta \eta x_{\eta|i}^{n+1} + \frac{1}{2!} \Delta \eta^2 x_{\eta\eta|i}^{n+1} + \frac{1}{3!} \Delta \eta^3 x_{\eta\eta\eta|i}^{n+1} \\ &\quad + \frac{1}{4!} \Delta \eta^4 x_{\eta\eta\eta\eta|i}^{n+1} + \dots, x_{i-1}^{n+1} \\ &= x_i^{n+1} - \Delta \eta x_{\eta|i}^{n+1} + \frac{1}{2!} \Delta \eta^2 x_{\eta\eta|i}^{n+1} - \frac{1}{3!} \Delta \eta^3 x_{\eta\eta\eta|i}^{n+1} \\ &\quad + \frac{1}{4!} \Delta \eta^4 x_{\eta\eta\eta\eta|i}^{n+1} - \dots \end{aligned}$$

Adding the above expressions and simplifying the results yield

$$\frac{x_{i+1}^{n+1} - 2x_i^{n+1} + x_{i-1}^{n+1}}{\Delta \eta^2} - x_{\eta\eta|i}^{n+1} = \frac{1}{12} \Delta \eta^2 x_{\eta\eta\eta\eta|i}^{n+1} + \frac{1}{360} \Delta \eta^4 x_{\eta\eta\eta\eta\eta\eta|i}^{n+1} + \dots,$$

where $\Delta \eta$ is the step size of the computational coordinates. Similarly, one can have

$$\tau \frac{x_i^{n+1} - x_i^n}{h_t} - \tau x_t = \frac{1}{2} h_t x_{tt|i}^n + \frac{1}{6} h_t^2 x_{ttt|i}^n + \dots$$

Thus, the truncation error of scheme (12) is

$$T_i^n = \tau \frac{x_i^{n+1} - x_i^n}{h_t} - \frac{x_{i+1}^{n+1} - 2x_i^{n+1} + x_{i-1}^{n+1}}{\Delta \eta^2} - (\tau x_t - x_{\eta\eta|i}^n).$$

Hence,

$$T_i^n = O(h_t) + O(\Delta \eta^2).$$

Similarly, we derive the accuracy of Eq. (13) by using Taylor series expansion to expand ψ_i^{n+1} and ψ_i^n . We consider a half of the time step size $h_t/2$, as follow:

$$\begin{aligned} \psi_i^{n+1} &= \psi_{|i}^{n+1/2} + \frac{h_t}{2} \psi_{t|i}^{n+1/2} + \frac{h_t^2}{8} \psi_{tt|i}^{n+1/2} + \frac{h_t^3}{48} \psi_{ttt|i}^{n+1/2} \\ &\quad + \frac{h_t^4}{348} \psi_{tttt|i}^{n+1/2} + \dots, \psi_i^n \\ &= \psi_{|i}^{n+1/2} - \frac{h_t}{2} \psi_{t|i}^{n+1/2} + \frac{h_t^2}{8} \psi_{tt|i}^{n+1/2} - \frac{h_t^3}{48} \psi_{ttt|i}^{n+1/2} \\ &\quad + \frac{h_t^4}{348} \psi_{tttt|i}^{n+1/2} + \dots \end{aligned}$$

Subtracting the above equations and simplifying the results lead to

$$\frac{\psi_i^{n+1} - \psi_i^n}{h_t} - \psi_t = \frac{h_t^2}{24} \psi_{ttt|i}^{n+1/2} + \frac{h_t^4}{1920} \psi_{tttt|i}^{n+1/2} + \dots$$

We now expand the spatial derivatives for ψ by using the average of finite differences at t_n and t_{n+1} as follows:

$$\begin{aligned} \psi_{i+1}^{n+1} &= \psi_i^{n+1} + \Delta x_{i+1} \psi_{x|i}^{n+1} + \frac{1}{2!} (\Delta x_{i+1})^2 \psi_{xx|i}^{n+1} + \frac{1}{3!} (\Delta x_{i+1})^3 \psi_{xxx|i}^{n+1} \\ &\quad + \frac{1}{4!} (\Delta x_{i+1})^4 \psi_{xxxx|i}^{n+1} + \dots, \psi_{i-1}^{n+1} \\ &= \psi_i^{n+1} - \Delta x_i \psi_{x|i}^{n+1} + \frac{1}{2} (\Delta x_i)^2 \psi_{xx|i}^{n+1} - \frac{1}{3!} (\Delta x_i)^3 \psi_{xxx|i}^{n+1} \\ &\quad + \frac{1}{4!} (\Delta x_i)^4 \psi_{xxxx|i}^{n+1} - \dots \end{aligned}$$

Let $h_x = \max(\Delta x_{i+1}, \Delta x_i)$. Then, we subtract the above expansions and simplifying the results to have

$$\frac{\psi_{i+1}^{n+1} - \psi_{i-1}^{n+1}}{2h_x} - \psi_{x|j}^{n+1} = \frac{1}{6} h_x^2 \psi^{(3)}(\xi)^{n+1},$$

where $\xi \in [x_{i-1}, x_{i+1}]$. Similarly, we deal with the second derivative as follows:

$$\frac{1}{h_x} \left(\frac{\psi_{i+1}^{n+1} - \psi_i^{n+1}}{h_x} - \frac{\psi_i^{n+1} - \psi_{i-1}^{n+1}}{h_x} \right) - \psi_{xx|i}^{n+1} = \frac{1}{24} h_x^2 \psi^{(4)}(\xi).$$

In a similar way, we can easily find the approximation of ψ_x and ψ_{xx} at the time level t_n . Therefore, the truncation error of the adaptive moving mesh Eq. (13) is given by

$$T_i^{n+1/2} = O(h_t^2) + O(h_x^2).$$

From this observations it could be simply concluded that the accuracy of the adaptive moving mesh method is much better than the accuracy which is from second-order because the spatial step size is much small in regions where the solution changes. Therefore, the truncation error can be expressed as

$$T_i^{n+1/2} = O(h_t^2) + O(\Delta x^2 |i^{n+1}).$$

5.2. Stability

We devote this part for the investigation of the stability of the numerical approximation (12) by using the Von Neumann analysis. The boundary conditions are ignored and we consider (t_n, η_m) with $t_n = n h_t$, and $\eta_i = i \Delta \eta$, $i = 0, \dots, N_x$. Eq. (12) can be written as

$$x_i^n = -\alpha x_{i+1}^{n+1} + (1 + 2\alpha)x_i^{n+1} - \alpha x_{i-1}^{n+1}, \tag{14}$$

where $\alpha = \frac{h_t}{\tau \Delta \eta^2} > 0$. In order to apply the Von Neumann technique, we assume that

$$x_i^n = \lambda^n \exp(i v \Delta \eta i), \tag{15}$$

where v is an arbitrary constant. Plugging Eq. (15) into Eq. (14) gives

$$1 = (1 - (\exp(i v \Delta \eta) - 2 + \exp(-i v \Delta \eta))) \lambda.$$

Since

$$\exp(i v \Delta \eta) - 2 + \exp(-i v \Delta \eta) = -4 \sin^2(0.5 v \Delta \eta),$$

one can obtain

$$|\lambda| = \frac{1}{|1 + 4 \alpha \sin^2(0.5 v \Delta \eta)|} \leq 1.$$

Hence, $0 \leq \lambda \leq 1$. As a result, Eq. (12) is unconditionally stable. Next, we examine the stability of scheme (13) by assuming that the mesh is uniform with an equal step size. Thus, the system is given by

$$\begin{aligned} \psi_i^{n+1} + r\gamma(\psi_{i+1}^{n+1} - \psi_{i-1}^{n+1}) + \frac{1}{3}\gamma(\psi_{xx|i+1}^{n+1} - \psi_{xx|i}^{n+1}) &= \psi_i^n + \\ r\gamma(\psi_{i+1}^n - \psi_{i-1}^n) - \frac{1}{3}\gamma(\psi_{xx|i+1}^n - \psi_{xx|i}^n), \end{aligned} \tag{16}$$

where $r = 0.75\psi_i^n - \mu$ and $\gamma = \frac{h_t}{4\Delta x}$. Let

$$\psi_i^n = \lambda^n e^{i v \Delta x i}. \tag{17}$$

Substituting Eq. (17) into scheme (16) leads to

$$\begin{aligned} \lambda \left(\frac{4}{\Delta x^2} \gamma \sin^2(0.5 v \Delta x)(1 - e^{i \Delta x}) + 6r\gamma \sin(v \Delta x) + 3 \right) \psi_i^n &= \\ - \left(\frac{4}{\Delta x^2} \gamma \sin^2(0.5 v \Delta x)(1 - e^{i \Delta x}) + 6r\gamma \sin(v \Delta x) - 3 \right) \psi_i^n \end{aligned} \tag{18}$$

Solving system (18) gives

$$|\lambda| = \frac{\left| \frac{4}{\Delta x^2} \gamma \sin^2(0.5 v \Delta x)(1 - e^{i \Delta x}) + 6r\gamma \sin(v \Delta x) - 3 \right|}{\left| \frac{4}{\Delta x^2} \gamma \sin^2(0.5 v \Delta x)(1 - e^{i \Delta x}) + 6r\gamma \sin(v \Delta x) + 3 \right|} \leq 1.$$

Since $|\lambda| \leq 1$, the scheme is unconditionally stable.

6. Results

We now highlight the significant results achieved in this work. The improved $\exp(-F(\eta))$ -expansion approach is successfully executed to extract various hyperbolic and trigonometric exact solutions for Eq. (1). Some solitary wave solutions are plotted in Figures 1, 2 and when $\beta = \delta = 1$ and $N = 400$. The shooting approach is effectively applied to solve the proposed problem. The obtained solution is used as an initial condition for the adaptive moving mesh technique which is implemented to construct the numerical results of Eq. (1). In Fig. 3, we plot the exact solitary traveling wave solution, the solution of the shooting method, and the solution of the boundary value problem method. As can be observed in this figure, the solutions are compatible and move together. This strongly indicates that the used method are reliable, valid, and effective.

Moreover, we specifically invoke Taylor series expansion to analyze the accuracy of the scheme. The accuracy is found from the second order. However, the accuracy of the proposed numerical approach is nearly from the third order, as can be seen in the slope of Fig. 7 which is roughly equal to 2.953. Therefore, the accuracy of the adaptive approach is much better than the accuracy of

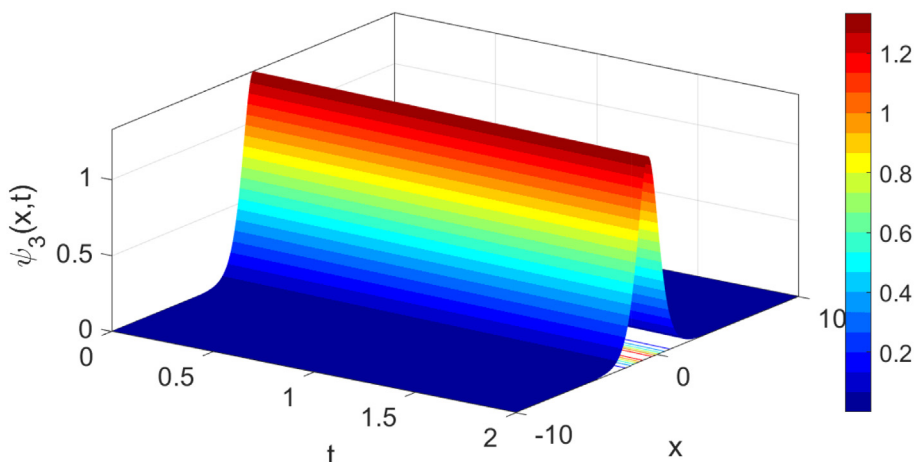


Fig. 1. A 3D surface sketching a single wave for the analytic solution $\psi_3(x, t)$ under the values $\beta = 1, \delta = 1$, and $N = 400$.

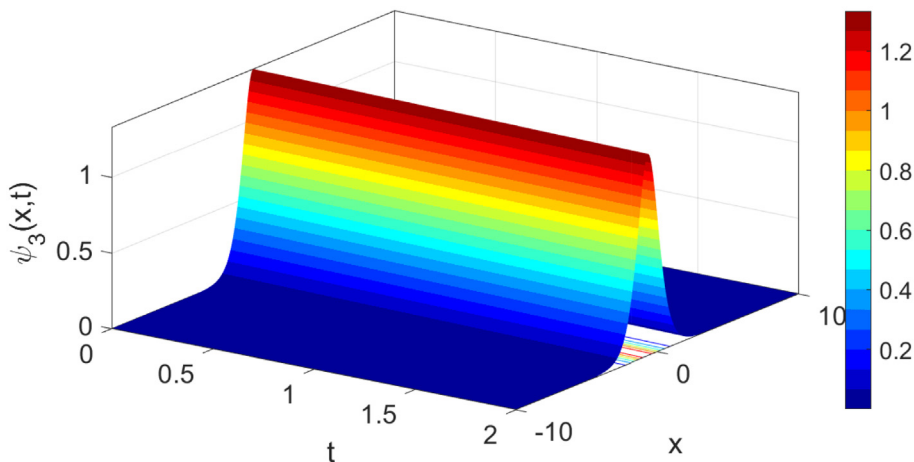


Fig. 2. The solitary wave solution of $\psi_3(x, t)$ when $\beta = 1, \delta = 1$, and $N = 400$.

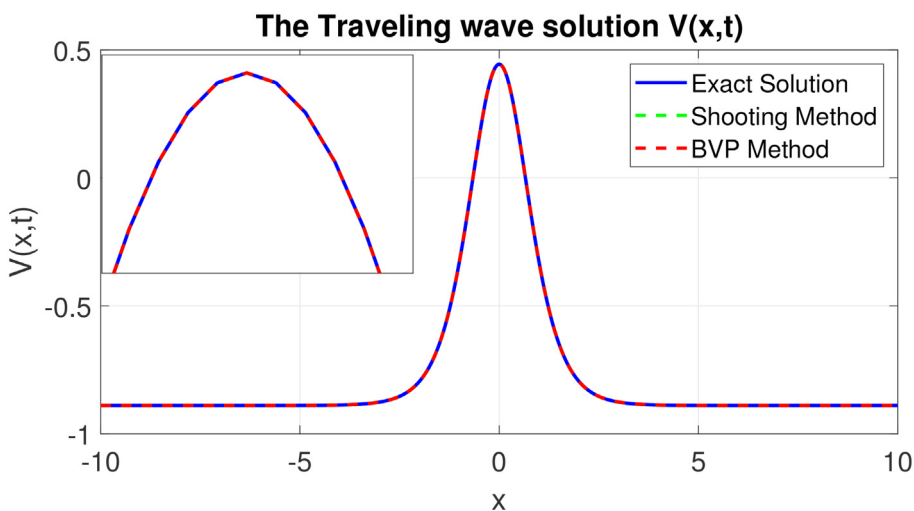


Fig. 3. The exact solution of $V(x, t)$ obtained by employing the improved $\exp(-F(\eta))$ -expansion technique, the solution obtained by shooting method and the numerical solution are compatible together. This figure is plotted under the values $\beta = 1, \delta = 1, N = 400$.

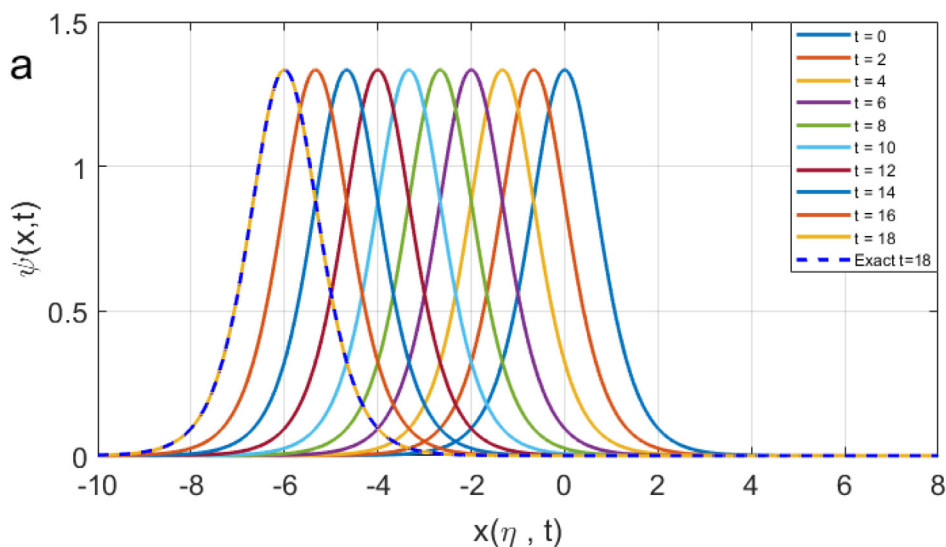


Fig. 4. Time development for the analytic and numerical solutions for $-10 < x < 8$. It shows an appropriate match between the exact and numerical solutions for various times. We use the values $\beta = 1, \delta = 1, N = 400, t = 0 : 0.5 : 2$, and $t = 2$ to sketch these figures.

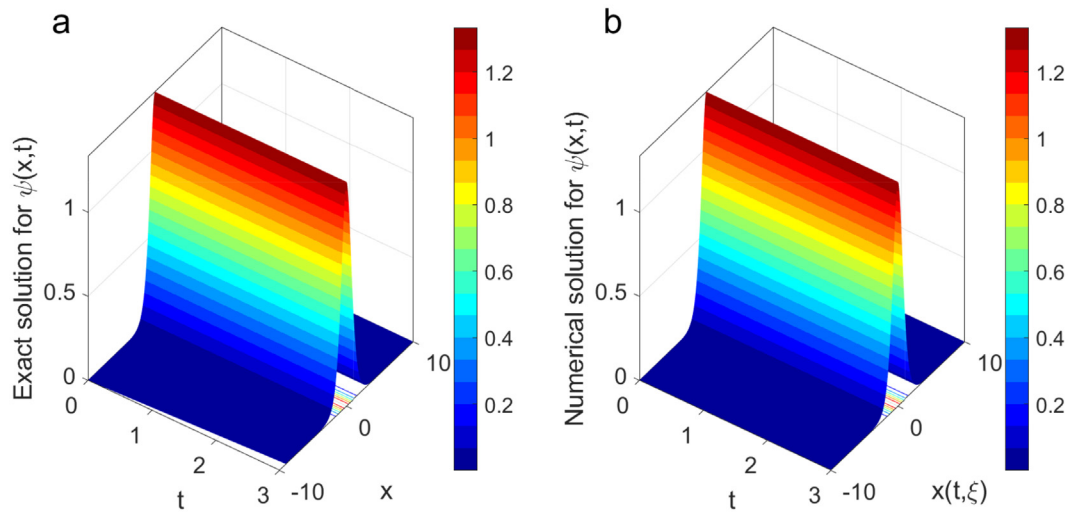


Fig. 5. The exact traveling wave solution is shown in (a) while the numerical solution is presented in (b). The solutions are plotted under the values $\beta = 1, \delta = 1, N = 400, t = 0 : 0.5 : 2, t = 0 \rightarrow 3$.

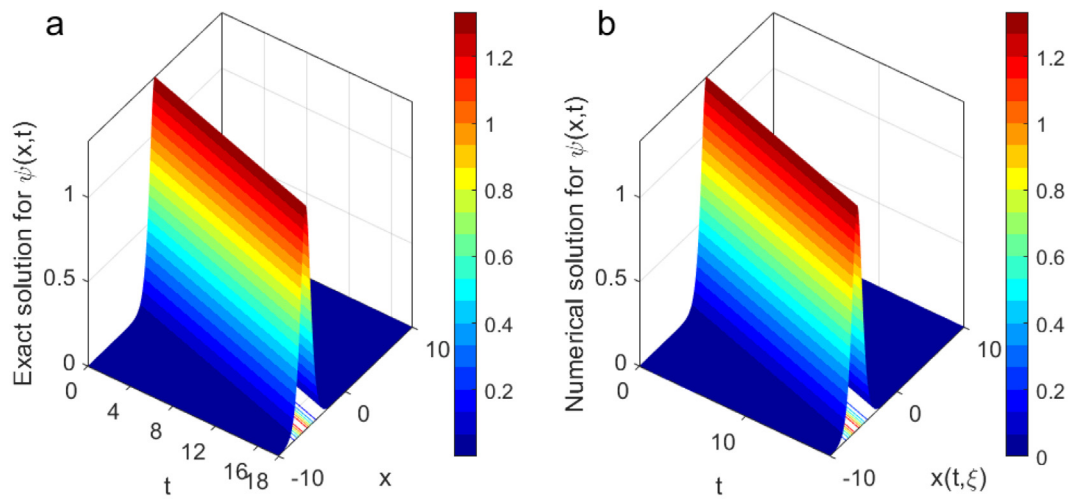


Fig. 6. A single traveling wave solution is depicted in (a) for the exact solution while (b) demonstrates one traveling wave for the numerical solution. The solutions are illustrated under the values $\beta = 1, \delta = 1, N = 400, t = 0 : 0.5 : 2, t = 0 \rightarrow 18$.

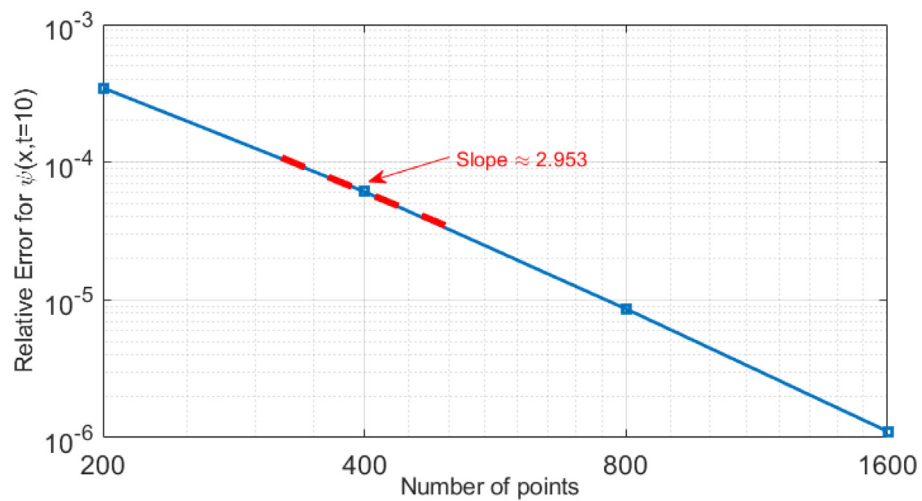


Fig. 7. Relative error for $\psi(x,t)$ which is found by the numerical method against the grid of points N_x with $\beta = 1, \delta = 1, t = 10$.

Table 1
 L_2 error and the consuming CPU time until $t = 5$.

N_x	L_2 error	CPU (minutes)
200	3.51×10^{-4}	5.23×10^{-2} m
400	6.11×10^{-5}	4.04×10^{-1} m
800	8.60×10^{-6}	$6.50 \times 10^{+00}$ m
1000	4.69×10^{-6}	$1.58 \times 10^{+1}$ m
1600	1.11×10^{-6}	$1.14 \times 10^{+2}$ m

the second order. Furthermore, the Von Neumann analysis is well used to prove that the numerical scheme is unconditionally stable. In Fig. 4, we draw the time evolution for the exact and numerical results for $-10 < x < 8$. Fig. 4(a) indicates that the constructed exact traveling solutions agree with the numerical solutions where $\beta = 1$, $\delta = 1$, and $N = 400$. Various times are considered in this figure. In Fig. 4(b), we describe the time evolution of the used mesh $x = x(\eta, t)$.

Fig. 5(a, b) show 3D plots for the obtained exact solitary traveling wave solutions and numerical solutions from $t = 0 \rightarrow 3$. Then, we increase time to be from $t = 0 \rightarrow 18$, as can be seen in Fig. 6 (a, b). As can be easily observed from these figures, the exact solutions have nearly the same behaviors of the numerical solutions. In addition, the effectiveness of the used methods is clearly shown in Table 1 and Fig. 7. In this table, we demonstrate L_2 error and CPU time consumed to reach $t = 5$ using the adaptive technique. We start with $N = 200$ points and found that L_2 error is virtually approaching 3.51×10^{-4} which is normally acceptable. The error decreases sharply when we increase the number of the points. Nevertheless, the CPU time increases somewhat when the number of the points is increased. For instance, when $N = 1600$, L_2 error arrives at 1.11×10^{-6} during $1.14 \times 10^{+2}$ minutes. The slight increment in the CPU time is for the reason that the used functions are computed with the process. Further, Fig. 7 presents that the relative error for $\psi(x, t = 10)$ dramatically drops for large values of the points. The error rapidly declines because the adaptive process supplies the places with high error by adequate and sufficient points. Consequently, the adaptive technique is more computationally powerful and applicable in solving nonlinear partial differential equations.

7. Conclusions

This paper has implemented the improved $\exp(-F(\eta))$ -expansion method on the gKdV equation to extract new forms of solitary wave solutions. The obtained solutions have been presented as hyperbolic and trigonometric functions. The shooting method has been used to construct the solution of the gKdV problem. Then, we used this solution as an initial condition for the adaptive moving mesh technique which has been successfully used to obtain the numerical solution of the proposed problem. The validation of the constructed solutions has been well achieved by making a comprehensive comparison between the analytic and numerical outcomes. The solutions have nearly the same behavior. The accuracy of the adaptive method is much better and is from the third order. The numerical scheme is found unconditional stable. Moreover, a large number of points reduces the relative error. The used techniques are computationally efficient to be employed on other nonlinear partial differential problems.

Declaration of Competing Interest

The authors declare that they have no known competing financial interests or personal relationships that could have appeared to influence the work reported in this paper.

References

- Abdullah, Seadawy Aly, Wang, R. Jun, 2019. Three-dimensional nonlinear extended Zakharov-Kuznetsov dynamical equation in a magnetized dusty plasma via acoustic solitary wave solutions. *Braz. J. Phys.* 49 (1), 67–78.
- Adjerid, Flaherty J.E., 1986. A moving finite element method with error estimation and refinement for one-dimensional time dependent partial differential equations. *SIAM J. Numer. Anal.* 23, 778–795.
- Adomain, G., 1994. Solving frontier problems of physics: The decomposition method. Kluwer Academic Publishers, Boston.
- Akbar, M.A., Akinyemi, L., Yao, Sh., et al., 2021. Soliton solutions to the Boussinesq equation through sine-Gordon method and Kudryashov method. *Results Phys.* 25, 104228.
- Ak, T., Saha, A., Dhawan, S., et al., 2020. Investigation of Coriolis effect on oceanic flows and its bifurcation via geophysical Korteweg-de Vries equation. *Numer. Methods Partial Differ. Eqs.* 36 (6), 1234–1253.
- Akinyemi, L., Nisar, K.S., Saleel, CA, et al., 2021. Novel approach to the analysis of fifth-order weakly nonlocal fractional Schrödinger equation with Caputo derivative. *Results Phys.* 31, 104958.
- Alam, M.N., Tunç, C., 2020. Constructions of the optical solitons and other solitons to the conformable fractional Zakharov-Kuznetsov equation with power law nonlinearity. *J. Taibah Univ. Sci.* 14 (1), 94–100.
- Alharbi, A.R., Almatrafi, M.B., 2020. New exact and numerical solutions with their stability for Ito integro-differential equation via Riccati-Bernoulli sub-ODE method. *J. Taibah Univ. Sci.* 14 (1), 1447–1456.
- Alharbi, A.R., Almatrafi, M.B., 2020. Numerical investigation of the dispersive long wave equation using an adaptive moving mesh method and its stability. *Results Phys.* 16, 102870.
- Alharbi, A.R., Almatrafi, M.B., 2020. Riccati-Bernoulli Sub-ODE approach on the partial differential equations and applications. *Int. J. Math. Comput. Sci.* 15 (1), 367–388.
- Alharbi, A.R., Almatrafi, M.B., Seadawy, A.R., 2020. Construction of the numerical and analytical wave solutions of the Joseph-Egri dynamical equation for the long waves in nonlinear dispersive systems. *Int. J. Mod. Phys. B*, 10. <https://doi.org/10.1142/S0217979220502896>, 2050289.
- Alharbi, A.R., Almatrafi, M.B., Lotfy, Kh., 2020. Constructions of solitary travelling wave solutions for Ito integro-differential equation arising in plasma physics. *Results Phys.* 19, 103533.
- Almatrafi, M.B., Alharbi, A.R., Tunç, C., 2020. Constructions of the soliton solutions to the good Boussinesq equation. *Adv. Differ. Equ.* 629. <https://doi.org/10.1186/s13662-020-03089-8>.
- Bekir, A., Unsal, O., 2012. Analytic treatment of nonlinear evolution equations using first integral method. *Pramana J. Phys.* 79 (1), 3–17.
- Chen, G., Xin, X., Liu, H., 2019. The improved $\exp(-\phi(\eta))$ -expansion method and new exact solutions of nonlinear evolution equations in mathematical physics. *Adv. Math. Phys.* Article ID 4354310, 8 pages. doi:10.1155/2019/4354310.
- El-Shiekh, R.M., Gaballah, M., 2020. Novel solitons and periodic wave solutions for Davey-Stewartson system with variable coefficients. *J. Taibah Univ. Sci.* 14 (1), 783–789.
- Geyer, A., Quirchmayr, R., 2017. Shallow water equations for equatorial tsunami waves. *Philos. Trans. R. Soc. A* 376, 20170100.
- Houwe, A., Abbagari, S., Inc, M., et al., 2022. Envelope solitons of the nonlinear discrete vertical dust grain oscillation in dusty plasma crystals. *Chaos Solitons Fractals* 155, 111640.
- Huang, W., Ren, Y., Russell, R.D., 1994. Moving mesh partial differential equations (MMPDEs) based on the equidistribution principle. *SIAM J. Numer. Anal.* 31, 709–730.
- Johnson, R.S., 2002. Camassa-Holm, Korteweg-de Vries and related models for water waves. *J. Fluid Mech.* 455, 63–82.
- Karunakar, P., Chakraverty, S., 2019. Effect of Coriolis constant on Geophysical Korteweg-de Vries equation. *J. Ocean Eng. Sci.* 4 (2), 113–121.
- Khater, M.M.A., Inc, M., Attia, R.A.M., et al., 2020. Abundant new computational wave solutions of the GM-DP-CH equation via two modified recent computational schemes. *J. Taibah Univ. Sci.* 14 (1), 1554–1562.
- Korteweg, D.J., Vries, G.D., 1895. XLI. On the change of form of long waves advancing in a rectangular canal, and on a new type of long stationary waves, the London. *Edinburgh Dublin Philos. Mag. J. Sci.* 39 (240), 422–443.
- Kudryashov, N.A., 2009. On new travelling wave solutions of the KdV and the KdV-Burgers equations. *Commun. Nonlinear Sci. Numer. Simul.* 14 (5), 1891–1900.
- Kumar, D., Seadawy, A.R., Joardar, A.K., 2018. Modified Kudryashov method via new exact solutions for some conformable fractional differential equations arising in mathematical biology. *Chin. J. Phys.* 56 (1), 75–85.
- Liu, J., Zhang, Y., 2018. Construction of lump soliton and mixed lump stripe solutions of $(3 + 1)$ -dimensional soliton equation. *Results Phys.* 10, 94–98.
- Martinez, H.Y., Khater, M.M.A., Rezazadeh, H., et al., 2021. Analytical novel solutions to the fractional optical dynamics in a medium with polynomial law nonlinearity and higher order dispersion with a new local fractional derivative. *Phys. Lett. A* 420, 127744.
- Nisar, K.S., Inan, I.E., Inc, M., et al., 2021. Properties of some higher-dimensional nonlinear Schrödinger equations. *Results Phys.* 31, 105073.
- Özkan, Y.S., Yaşar, E., Seadawy, A.R., 2020. A third-order nonlinear Schrödinger equation: the exact solutions, group-invariant solutions and conservation laws. *J. Taibah Univ. Sci.* 14 (1), 585–597.
- Rao, J., Mihalache, D., Cheng, Y., He, J., 2019. Lump-soliton solutions to the Fokas system. *Phys. Lett. A* 383 (11), 1138–1142.

- Rizvi, S.T.R., Seadawy, A., Ashraf, F., et al., 2020. Lump and Interaction solutions of a geophysical Korteweg-de Vries equation. *Results Phys.* 19, 103661.
- Shampine, L., Reichelt, M., 1994. The matlab ode suite. *SIAM J. Scientific Comput.* 18, 1–22.
- Triki, H., Ak, T., Biswas, A., 2017. New types of soliton-like solutions for a second order wave equation of Korteweg-de Vries type. *Appl. Comput. Math.* 16 (2), 168–176.
- Wang, M.L., Zhou, Y.B., Li, Z.B., 1996. Application of a homogeneous balance method to exact solutions of nonlinear equations in mathematical physics. *Phys. Lett. A* 216, 67–75.
- Wazwaz, A.M., 2002. *Partial differential equations: method and applications*. Taylor and Francis.
- Wazwaz, A.M., 2010. Multiple-soliton solutions of the perturbed KdV equation. *Commun. Nonlinear Sci. Numer. Simul.* 15 (11), 3270–3273.
- Wazzan, L., 2009. A modified tanh-coth method for solving the KdV and the KdV-Burgers' equations. *Commun. Nonlinear Sci. Numer. Simul.* 14 (2), 443–450.
- Zafar, A., Shakeel, M., Ali, A., et al., 2022. Optical solitons of nonlinear complex Ginzburg-Landau equation via two modified expansion schemes. *Opt. Quant. Electron.* 54 (5). <https://doi.org/10.1007/s11082-021-03393-x>.